

# Characteristics of Pneumatic Atomization

JAMES GRETZINGER and W. R. MARSHALL, JR.

University of Wisconsin, Madison, Wisconsin

The widespread applications of sprays to problems in industry and agriculture involve a variety of spray producing devices. The characterization of these sprays often includes the measurement of an average drop size or drop-size distribution and a spatial distribution of the spray droplets. These properties of sprays are functions of the spray producing device, the manner in which the device is used, and the nature of the liquid sprayed. This paper considers sprays produced by the disruptive action of a high velocity air stream on thin liquid films or filaments. This method of spraying is commonly known as *pneumatic atomization* or *two-fluid atomization*. The former term is to be preferred, since the latter can include two liquid streams.

Pneumatic nozzles are well suited to the production of sprays with average drop diameters in the less than 30  $\mu$  range. However this is usually accomplished at relatively modest capacities, on the order of a few gallons per hour; this limits their widespread use. By contrast pressure nozzles and rotating disk atomizers are extensively used to form sprays having average drop diameters in the 75 to 1,000  $\mu$  range and greater. The drop sizes covered in this study ranged from 5 to 30  $\mu$ . In the course of the experimental work two types of pneumatic atomizers designed for spray drying operations were evaluated.

## SOME PREVIOUS WORK

Probably the best known and most widely quoted research in pneumatic atomization is that of Nukiyama and Tanasawa (1). Their studies resulted in the following equation which related the Sauter mean drop diameter to the gas and liquid rates and liquid properties:

$$\bar{x}_{rs} = \frac{585}{v} \sqrt{\frac{s}{\rho}} + 597 \left( \frac{\mu}{s\rho} \right)^{0.45} \left( \frac{1,000 Q_l}{Q_a} \right)^{1.5} \quad (1)$$

Equation (1) is limited to small nozzles of a specific design and to a rather small range of capacities.

Analysis of the Nukiyama and Tanasawa equation shows that for ratios of  $Q_a$  to  $Q_l$  greater than 5,000 the second term in the right-hand side of the equation

contributes very little to the predicted drop size for most low viscosity liquids. Since the relative velocity of gas to liquid generally approaches sonic velocity at a  $Q_a/Q_l$  of 5,000 for most nozzles, the value of the predicted drop size approaches a constant which depends primarily on liquid density and surface tension. On the basis of these observations and the description of the Nukiyama and Tanasawa experimental technique (1) one concludes that application of the equation to atomization for a size range of 5 to 30  $\mu$  is of doubtful value.

A comparison of literature data on pneumatic atomization is summarized in Figure 1. The wide spread of the data on the mass median drop size as a function of gas-to-liquid mass ratio is a striking feature of this graph. It is evident that a full understanding of pneumatic atomization demands an explanation for the wide variation of drop size as a function of gas-to-liquid mass ratio and atomizer design.

Radcliffe and Clare (2), using a technique developed by Joyce (3), studied the drop sizes produced by two air-blast nozzles (pneumatic atomizers in which the atomizing air was caused to rotate prior to contacting the liquid). Their correlations indicated that the mass median drop size varied inversely with the mass ratio of atomizing air to liquid.

Kim (4) reported the drop size of sprays of aqueous sodium sulfate solution, produced by a converging pneumatic nozzle. The linear velocity of atomizing air was less than sonic velocity at all points in his atomizer.

Garner and Henry (5) reported drop-size data for pneumatic atomization of petroleum ether, ethyl alcohol, and several liquid hydrocarbons. Their sprays were formed in chambers held at subatmospheric pressures. Their data indicated an inverse variation of spray particle size in the range 30 to 17  $\mu$  for air to liquid ratios in the range 1.2 to 9.0.

Golitzine et al. (6) atomized water with air and observed an inverse variation of drop size in the range 40 to 12  $\mu$  with air to liquid mass ratios in the range 1.5 to 10. Spray drop size was found to be a function of nozzle dimensions.

Anson (7) atomized kerosene with a pneumatic nozzle and observed an inverse variation of drop size in the range 150  $\mu$  to 60  $\mu$  with air to fuel mass ratios in the range of 20 to 30.

Wetzel (8) studied venturi atomization of a molten wax and a molten metal alloy with room temperature air. Again the inverse variation of drop size in the range 110 to 30  $\mu$  with air-to-liquid mass ratios of 100 to 300 was found.

Bitron (9) studied the breakup of a dibutyl phthalate stream contacted at right angles by air at supersonic velocity. Drop-size variation with gas-to-liquid mass ratio was not observed; the atomizer design and operating conditions undoubtedly account for this effect. The data of Lewis et al. (9a) are given for completeness, but there is serious question regarding the reliability of their drop sampling technique.

In Figure 2 sectional views are shown of some of the pneumatic nozzles used by the investigators mentioned. The

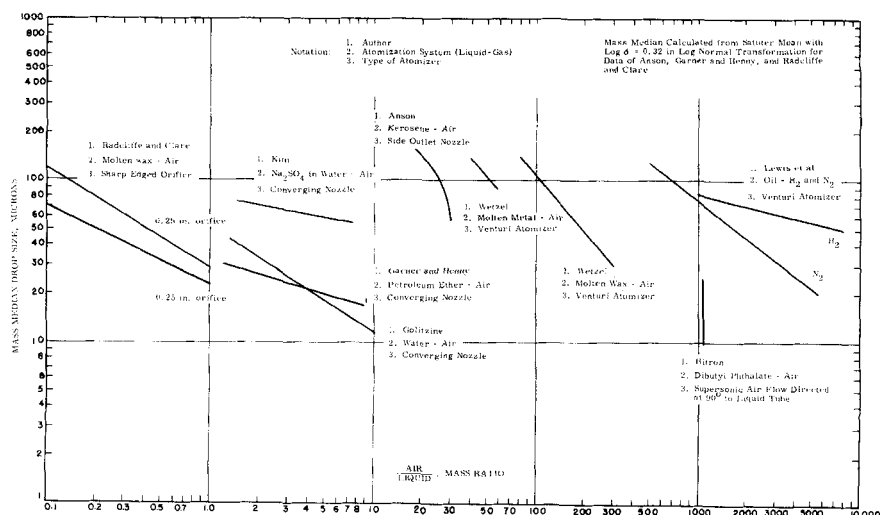


Fig. 1. Pneumatic atomization reported by other workers.

James Gretzinger is at E. I. du Pont de Nemours and Company, Buffalo, New York.

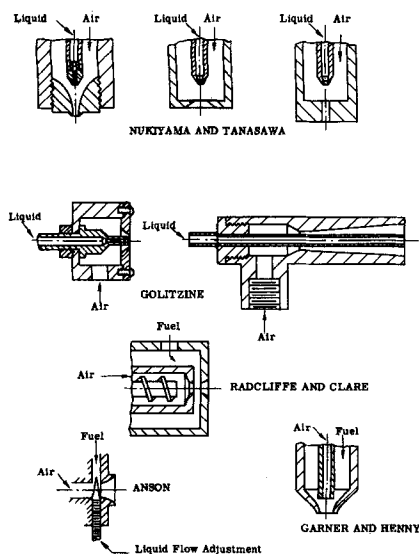


Fig. 2. Nozzle designs.

numerous configurations for bringing liquid and air streams together is indicated. Air and liquid contacting can be accomplished within the nozzle, at the nozzle exit, or outside the nozzle. The fluid streams can meet either at right angles or in concurrent flow. Spin can be imparted to either or both streams in some designs. These designs by no means exhaust the possibilities; they merely suggest a few of the multiplicity of nozzle shapes that have been devised and investigated.

The lack of a suitable atomization theory, the numerous designs of pneumatic atomizers available, and the many techniques for drop size analysis, many unreliable and uncertain, have all contributed to a state of confusion in this field. From an engineering standpoint some of the questions that must be answered are:

1. What is the interaction of air and liquid streams or films during atomization?
2. How do liquid properties affect the interaction of air and liquid?
3. How do air stream properties affect pneumatic atomization?
4. What is the most effective means for contacting air and liquid for atomization purposes?
5. What are the power requirements and efficiency of power consumption in pneumatic atomization?

## EXPERIMENTAL PROCEDURES

### Nozzles

Although a number of different types of pneumatic nozzles were employed during the course of this work, most of the drop-size data were obtained with a converging pneumatic nozzle and a pneumatic impingement nozzle, shown in Figures 3 and 4 respectively. These nozzles were chosen because they permitted studies of

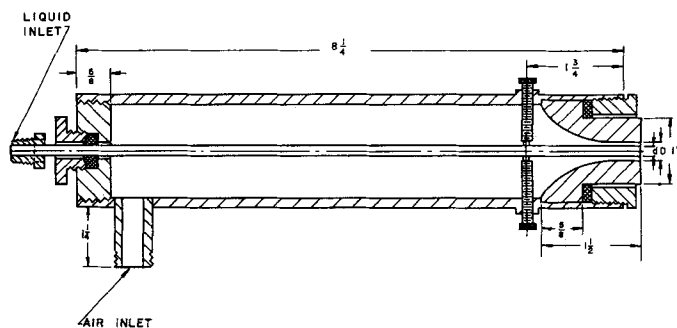


Fig. 3. Converging pneumatic nozzle.

contrasting spray patterns and the effect of a range of nozzle insert sizes.

In the converging pneumatic nozzle, Figure 3, the liquid feed tube terminated at the minimum diameter of a converging nozzle for the air stream. Thus liquid in the form of a thin cylindrical shell was drawn from the central tube and broken up by the surrounding high velocity air stream emerging as an exterior annulus from the converging section of the nozzle. Several combinations of feed tubes and converging inserts were used as given in Table 1.

The pneumatic impingement nozzle, Figure 4, was made of two concentric tubes. The innermost tube was the air conduit; the annular space between the tubes was the liquid conduit. Each tube was fitted with converging outlet pieces. The outer converging piece brought the liquid to the surface of the outlet of the air tube nozzle. An impinger, mounted on a rod centered in the air tube, permitted adjustment of the air flow pattern and produced corresponding changes in the spray cone angle. During this study the impinger was set at a distance of  $\frac{1}{4}$  in. from the face of the air orifice. Three air orifices of 0.094; 0.110; and 0.125-in. diameters were employed.

### Photographic Techniques

To aid in understanding the flow behavior of high-velocity air relative to the atomization process air flow patterns from the two nozzles were observed by a shadowgraph technique. This technique is described by Dvorak (10) and Foley (11).

High-speed photographs of water sprays

produced by pneumatic atomization were taken with a camera with illumination from a source having a peak duration of  $2 \mu$  sec. Although interesting and informative photographs were obtained, it was evident that even greater speed was necessary to stop motion during pneumatic atomization. This was especially true if magnification were needed to improve definition of the atomization mechanism.

### Particle-Size Measurement

In the initial phases of this work several methods of direct spray sampling were tried. However attempts to collect representative samples of fine sprays of water, aniline, dibutyl phthalate, and benzyl benzoate indicated that the lifetime of drops in the 1-to 15- $\mu$  diameter range was extremely short even though the vapor pressures of the liquids were as low as  $1.1 \times 10^{-4}$  mm. of mercury at 18°C. Twort et al. (12) and Whytlaw-Gray and Patterson (14) reported measurement of droplet disappearance rates in still air using a procedure similar to the Millikan oil-drop technique. Drops having diameters from 2 to 20  $\mu$  lasted less than 1.2 min. in the case of benzyl benzoate and 0.06 sec. for water. Thus an accurate means for measuring the size of very small drops, that was insensitive to evaporation, had to be developed.

Preservation of water drops by collection in materials such as mineral oil proved unreliable. It was observed that 15-to 20- $\mu$  water drops, collected on mineral oil coated microscope slides, disappeared completely in less than a minute.

A new technique was developed in this study to obtain spray drop sizes from

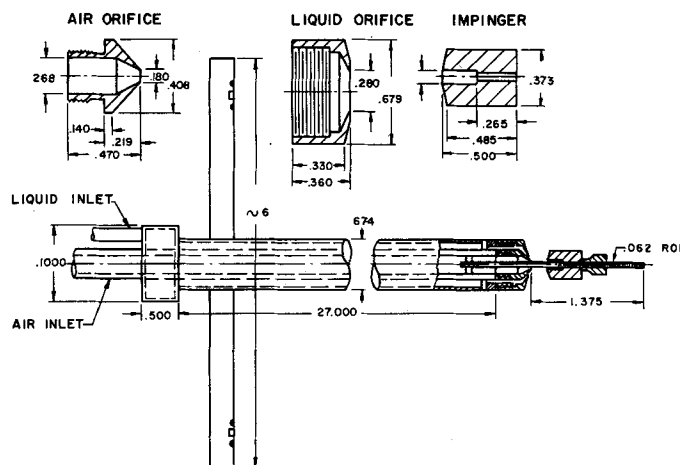


Fig. 4. Pneumatic impingement nozzle.

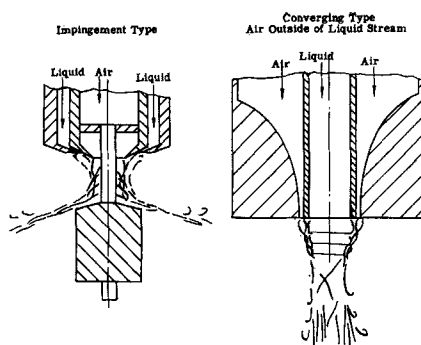


Fig. 5. Flow patterns of pneumatic atomizers.

pneumatic atomizers. The method consisted of (1) forming the fine spray from an aqueous solution of a black dye, (2) evaporating the water from the droplets, (3) collecting a sample of the resultant dye aerosol in mineral oil, (4) counting the dye particles with the aid of a light microscope, (5) plotting the number frequency distributions of the dye particles, and (6) calculating the mass distribution of the original spray droplets from the dye particle number distribution, the density of the dye particles, and the original concentration of dye in the liquid sprayed. In step 6 the dye particle-water drop material-balance relationship was developed on the basis of an individual drop and then applied to the median size of the drop distribution. Considering a liquid drop of diameter  $x_i$  containing  $C$  g./ml. of dye one can designate the resulting dried drop (dye particle) by a diameter  $x_s$  whose density is  $\rho_s$ . Since the mass of solid remains constant during the drying process, a material balance can be written as

$$\frac{\pi}{6} x_i^3 C = \frac{\pi}{6} x_s^3 \rho_s \quad (2)$$

This equation can be rearranged to give Equation (3):

$$x_s \left( \frac{\rho_s}{C} \right)^{1/3} = x_i \quad (3)$$

If the particle density is independent of particle size, and if the dry product has a logarithmic normal distribution with a mass median  $(\bar{x}_m)_s$  and a standard deviation  $\sigma_m$ , then the original spray must also have a logarithmic normal distribution with the same standard deviation and a mass median diameter  $(\bar{x}_m)_i$ . The mass median diameter of the dry product was calculated from the number median and standard deviation of the dry product by means of the following relationship:

$$\log (\bar{x}_m)_s = \log (\bar{x}_m)_i + 6.909 \log^2 \sigma_m \quad (4)$$

Conversion of the mass median diameter of the dry-product distribution to the mass median diameter of the original spray was

made by means of Equation (3), where  $x_s$  was replaced with  $(\bar{x}_m)_s$  and  $x_i$  was replaced by  $(\bar{x}_m)_i$ . The quantity  $\left( \frac{\rho_s}{C} \right)^{1/3}$  was the conversion factor between the mass median diameter of the dry product and the mass median diameter of the spray.

The drop size analysis technique was first tested with a medical nebulizer. Preliminary studies with a cascade impactor indicated that the mass median drop diameter of nebulizer sprays was in the 8-to 15- $\mu$  range. Replicate size analyses of these sprays measured by the material-balance method indicated good agreement for both the mass median particle size and the geometric standard deviation. On this basis it seemed reasonable that the method could be extended to drop-size distributions obtained with pneumatic atomizers producing sprays having a mass median diameter greater than 6  $\mu$  and liquid capacities up to 5 gal./hr.

Sprays from pneumatic nozzles, which were to be studied by the material-balance method, were produced in a spray dryer. Each dye aerosol so produced was sampled at the outlet of the spray dryer by collection in mineral oil with a high-efficiency impinger similar to that used by Rosebury (15). Samples of the mineral oil and dye particles were taken, microscope slides were prepared from these samples, and the dye particles were measured and counted by direct observation with a microscope. Magnifications ranging from 2,217 X to 2,720 X were used. For each data point 1,200 to 3,000 particles were counted and classified in size increments of 0.5 or 0.6  $\mu$ . All dye particle distributions followed a logarithmic normal distribution law.

Some particle-size analyses were also made with the liquid-wax technique of Joyce (3) to compare the results obtained with the material-balance method.

## EXPERIMENTAL RESULTS

Sketches of shadowgraphs of air-flow patterns photographed with each nozzle are shown in Figure 5. The air flow from the pneumatic impingement nozzle suggested that liquid or spray traveled along the outside of the air pattern and followed a rapidly diverging, conical path. This condition varied with the position of the impinger and the applied air pressure. It seemed reasonable to assume that this resulted in very effective use of the energy of the expanding air stream to break the liquid film into small and relatively uniform drops. The expansion pattern for the converging nozzle did not allow liquid or spray to contact the high velocity air

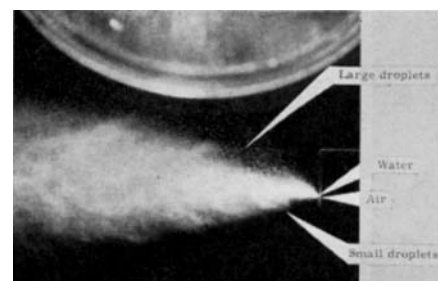


Fig. 6. Nonuniform atomization with air flow on one side only of a flat liquid sheet.

stream over as long a path as that of the impingement nozzle type.

A series of shadowgraphs taken of each nozzle at successively higher air pressures indicated that air-flow patterns had nodes of increasingly greater wave length and that the number of stable nodes increased with air pressure.

During the shadowgraph study it was noticed that expansion patterns for the air streams were visible to the naked eye when they were observed from the proper angle and when air supply pressures were at least 60 lb/sq. in. gauge. Observations of the converging pneumatic nozzle showed that lack of concentricity of the liquid feed tube and the air orifice greatly altered the air flow pattern. In early drop-size experiments irregular air-flow patterns gave nonreproducible results. After this observation was made, four set screws were installed on the nozzle to provide for careful adjustment to ensure the necessary concentricity of feed tube and air orifice. Shadowgraphs of air flow from a commercial converging nozzle

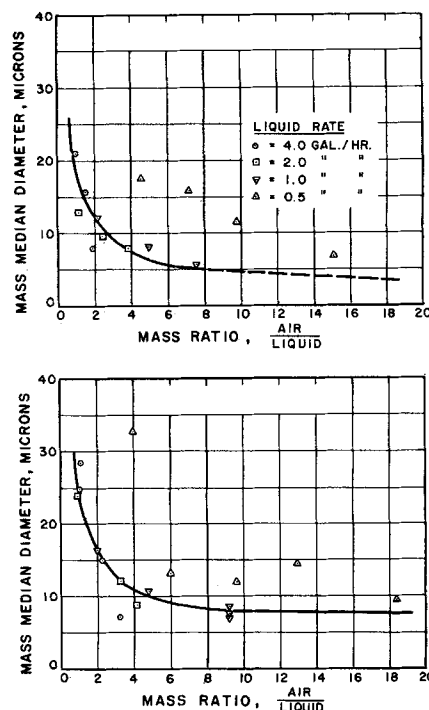


Fig. 7. Pneumatic impingement nozzle.

TABLE 1. CONVERGING PNEUMATIC NOZZLE INSERT COMBINATIONS

Insert series number	Diameter of converging air nozzle, in.	Liquid tube outside diameter, in.	Liquid tube inside diameter, in.	Area of air annulus, sq. in.
I	0.145	0.072	0.054	0.0124
II	0.205	0.163	0.125	0.0121
III	0.279	0.250	0.217	0.0120

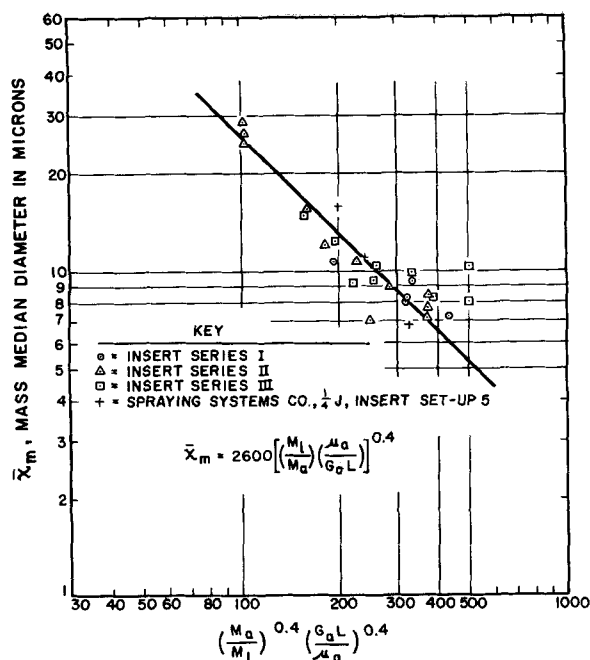


Fig. 8. Converging pneumatic nozzle correlation.

and the one designed during this study showed markedly similar air-flow patterns even though the internal passages of the nozzles differed.

To supplement the shadowgraph studies of the air-flow patterns a photographic study was made of the atomizers to determine the configuration of the air and liquid streams flowing simultaneously. Photographs were made of the converging pneumatic nozzle operating at various air pressures and liquid flow rates with standard low-speed illumination. These photographs indicated that the liquid flow which was interior to the air flow, closely followed the inside of the air-flow pattern. In those cases where the air flow had a definite scalloped effect on the interior, as indicated by the shadowgraph studies, the spray pattern was found to duplicate exactly this effect. It is interesting to note that the wave length of the air-flow pattern was constant at 0.08 in. for liquid feed rates from 0.5 to 4.5 gal./hr. and air pressures from 80 to 100 lb./sq. in. gauge. Thus it was concluded that liquid flow rate in the range studied had relatively little effect on air-flow pattern in the vicinity of the nozzle outlet at a given air-supply pressure. Typical patterns of the combined flow of air and liquid from the pneumatic atomizers are shown in Figure 5. For the impinging nozzle the liquid followed the outside surface of the interior air stream but never penetrated it at the impinger. As a result it traveled radially outward at the impinger without coming in contact with it.

An attempt was made to photograph the mechanism of pneumatic atomization by means of high speed, high intensity illumination techniques. A spe-

cial nozzle was designed and constructed for the purpose of bringing into contact concurrent, flat sheets of liquid and high-velocity air. The contact width of the air and liquid sheets and the area of the air-expansion slot were made to conform with the values of converging nozzle Series II inserts, Table 1. Photographs of this nozzle showed that high-speed illumination, 2- $\mu$ sec. peak duration, was not fast enough to stop all action during atomization of the liquid. The photographs indicated however that the smallest drops in a given spray were formed on the side of the liquid sheet in intimate contact with the gas stream, as shown in Figure 6. Large drops were formed on the opposite side of the liquid sheet and moved away from the air stream slowly and in a stable condition. These observations served to emphasize the need for uni-

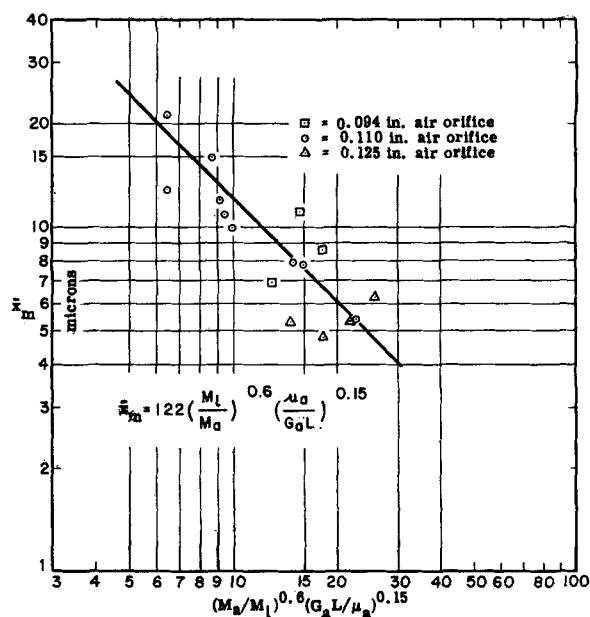


Fig. 9. Pneumatic impingement nozzle correlation.

formly contacting a liquid sheet on both sides if uniform breakup is to be achieved.

#### Drop-Size Data

The mass median diameters of sprays produced with the converging pneumatic nozzle and the pneumatic impingement nozzle were found to vary significantly with the mass ratio of atomizing air to liquid atomized. For each nozzle the mass median drop-size data could be fitted with a hyperbola as long as the data were taken at liquid rates of 1 gal./hr. or greater. Operation of the converging nozzle at a liquid rate of 1/2 gal./hr. resulted in unstable, pulsating spray flow. The drop sizes for the latter flow rate were somewhat greater than the values expected on the basis of the hyperbolic curve; this is shown in Figure 7 for both the converging and impinging nozzles.

When the drop-size data were plotted on log-log paper, separate lines were

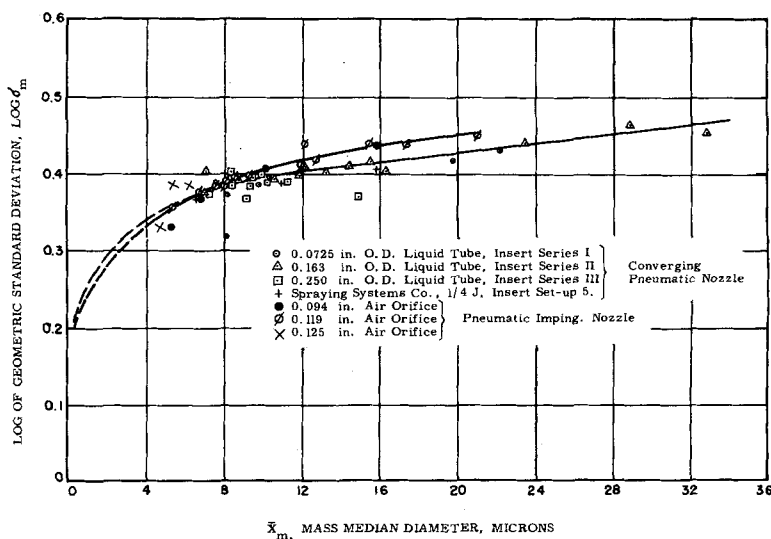


Fig. 10. Variation of standard deviation with mass median diameter.

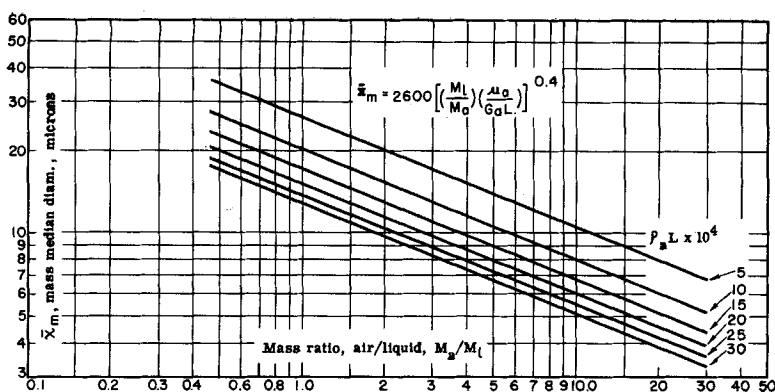


Fig. 11. Converging pneumatic nozzle correlation chart. The parameter is  $P_a L \times 10^4$  cm.-g./cc.

obtained for each insert series of each nozzle. It was apparent that spray mass median diameter varied with nozzle size as well as mass ratio of air to liquid flow. In the case of the converging nozzle the spray mass median diameter, at a given mass ratio of air to liquid, decreased as the liquid tube diameter increased. This was interpreted to mean that the liquid was spread over a greater exit perimeter resulting in a decrease in the liquid film thickness. The energy of the air stream was most effectively used when the thinnest liquid film was presented. A similar trend occurred for the pneumatic impingement nozzle. The spray drop size decreased as the air orifice size was increased up to 0.125 in., at which size the trend ceased.

The drop size data for each nozzle were correlated as a function of mass ratio of the air and liquid streams, the product of air mass velocity at the nozzle outlet, and the diameter of the contact periphery of the air and gas streams. The viscosity of the air in the outlet of the nozzle was not systematically studied. Figures 8 and 9 show the correlations for mass median diameters for each nozzle. Equations obtained from the graphs are:

*Converging Pneumatic Nozzle.*

$$\bar{x}_m = 2600 \left[ \left( \frac{M_l}{M_a} \right) \left( \frac{\mu_a}{G_a L} \right) \right]^{0.4} \quad (5)$$

*Pneumatic Impinging Nozzle.*

$$\bar{x}_m = 122 \left( \frac{M_l}{M_a} \right)^{0.6} \left( \frac{\mu_a}{G_a L} \right)^{0.15} \quad (6)$$

Since at the outlet of each nozzle the air was travelling at sonic velocity in all runs, the mass velocity term reflects the effect of air density on drop size.

To determine the extent to which Equation (5) could be generalized a round spray pneumatic nozzle was tested with a standard number 5 insert. Drop-size data obtained in three runs with this nozzle are shown in Figure 8. The three data points obtained fit the correlation reasonably well. It was interesting to note that the shadowgraph pattern for the nozzle was quite similar to that obtained for the converging

pneumatic nozzle. From this similarity it might have been predicted that the drop-size data would fit the correlation.

The technique of atomizing liquid wax was used with the converging pneumatic nozzle. The drop-size data obtained by this method were found to agree with the converging nozzle correlation, Figure 8.

The spread of the drop-size distributions formed by the nozzles was expressed by the log of the geometric standard deviation  $\sigma_m$ . Figure 10 gives curves of  $\log \sigma_m$  as a function of mass median drop size for each nozzle. These curves, plotted on log-log coordinates, led to Equations (7) and (8):

*Converging Nozzle.*

$$\sigma_m = 1.77 \bar{x}_m^{0.14} \quad (7)$$

*Pneumatic Impinging Nozzle.*

$$\sigma_m = 1.735 \bar{x}_m^{0.16} \quad (8)$$

#### Limitations of Drop Size Correlations

With Equations (5), (6), (7), and (8) it is possible to predict the mass median diameter and geometric standard deviation of drop-size distributions in sprays formed by either a converging nozzle or an impingement nozzle. It is not known however to what extent either series of equations may be used beyond the limits of the experimental data, that is drop mass median diameters from 5 to 29  $\mu$  and liquid rates from 0.5 to 5 gal./hr.

The correlations are specific to the two nozzle types studied; their application to other nozzle types must be done with discretion. It is possible that the converging nozzle correlation may give satisfactory results with the Nukiyama and Tanasawa nozzles shown in Figure 2. The accuracy of results would of course be dependent upon proper selection of values of air density and of the diameter of the air-liquid contact periphery. On the other hand one would not expect satisfactory results for a nozzle in which the gas and liquid streams met in other than a concurrent fashion. This is particularly true for nozzles in which the expanding air stream and the liquid stream meet at right angles.

The effect of liquid properties on drop sizes produced by pneumatic atomization was not investigated. As a result the correlations are limited to fluids whose physical properties are similar to those used in the tests. Satisfactory results should be obtainable with liquids having viscosities close to 1 centipoise and surface tensions in the range of 50 dynes/cm. Other limitations are as follows: mass ratios of air to liquid between 1 and 15; liquid film thicknesses between 0.3 and 0.6 mm., film thicknesses were calculated by the method of Friedman and Miller (13); gas at sonic velocity in the nozzle discharge port; and gas densities in the nozzle discharge port between  $2 \times 10^{-8}$  to  $5 \times 10^{-8}$  g./cc.

It should not be concluded that the correlations are entirely invalid beyond the ranges mentioned. However their accuracy outside of the specified limits has not been tested. In a test with molten wax with a viscosity of 7.5 centipoises, atomized with the converging nozzle, it was found that the drop size obtained fit the correlation. This suggests that correlations might hold for viscosities somewhat greater than water. It is also of interest that the data of Radcliffe and Clare (2) appeared to extend the converging nozzle data to mass ratios of air-to-liquid of less than 1. Since Radcliffe and Clare made their studies by

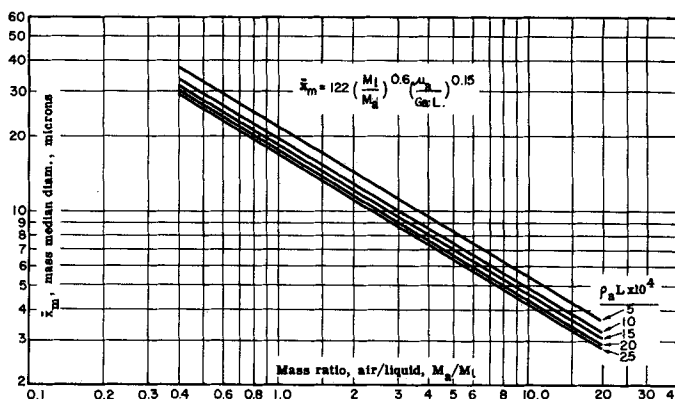


Fig. 12. Pneumatic impingement nozzle correlation chart. The parameter is  $P_a L \times 10^4$  cm.-g./cc.

TABLE 2. CALCULATED VALUES FOR EXAMPLE PROBLEM

Con- dition	$M_a/M_l$	$\rho_a L \times 10^4$ g./sq. cm.	$L$ , cm.	Liquid tube I.D., cm.	$N_{Re}$ , liquid	Liquid film thickness, cm.
A	0.70	30	1.000	0.900	130.3	0.020
B	0.82	25	0.833	0.733	159.8	0.022
C	1.03	20	0.677	0.567	206.6	0.023
D	1.40	15	0.500	0.400	293.0	0.026
E	2.10	10	0.333	0.233	503.0	0.031
F	4.20	5	0.167	0.067	1,750.0	

Final design con- dition	$M_a$ , lb./min.	$M_a$ , lb./sec.	Air flow area, sq. in.	Air annulus, O.D. in.	Liquid tube, O.D. in.	Liquid tube, I.D. in.	Air supply pressure, lb./sq. in. abs.
E	0.582	0.0097	0.006549	0.182	0.131	0.091	68.0

the molten-wax technique, their data also suggest that Equations (5), (6), (7), and (8) might be safely extended to liquid viscosities as high as 30 centipoises.

#### Application of Experimental Results

Application of Equations (5) to (8) is not as straightforward as one might suspect at first glance. To clarify the use of these equations correlation charts have been prepared and an example design problem carried out.

**Correlation Charts.** Design graphs of the drop-size correlations given by Equations (5) and (6) are given in Figures 11 and 12. In each figure the spray mass median drop diameter has been plotted vs. the mass ratio of the air and liquid flow rates  $M_a/M_l$ . The factor  $\rho_a L$  denoting the product of air density at the nozzle outlet and the diameter of the air-to-liquid contact periphery was used as a parameter. Metric units were used for  $x_m$  and  $\rho_a L$ .

Each chart contains a family of curves that can be used to calculate the range of variables necessary to produce required spray mass median diameters.

It is of interest to note that  $\rho_a L$  has a greater effect on the converging nozzle than on the impingement one.

**Example Design Problem**—This illustrates a procedure for designing a converging pneumatic nozzle to produce a spray at a given rate with a specified mass median diameter. The steps to follow are:

1. State the problem in terms of median drop size and liquid flow rate desired.
2. Use Figure 11 to obtain a set of values of  $M_a/M_l$  and  $\rho_a L$  which can be used to produce the desired median drop size.
3. Assume values for air density and temperature at nozzle exit and select a wall thickness for the liquid tube.
4. Calculate values of  $L$  and tabulate the inside diameters of possible liquid tube sizes.
5. Calculate the Reynolds number and liquid film thickness of the liquid flow in each liquid tube size by the method of Friedman and Miller (13).
6. Eliminate those values of  $M_a/M_l$  and  $\rho_a L$  for which the film thickness is less than 0.3 mm. or the Reynolds number of the liquid flow is greater than 1,000.
7. For the remaining

conditions calculate the mass of air necessary, the outside diameter of the air annulus, and the air supply pressure required. 8. Using Equation (7) calculate the geometric standard deviation of the spray.

The example follows the steps outlined above. The calculated values are presented in Table 2.

**Step 1**—It is desired to atomize a fluid whose properties are very similar to those of water at the rate of 2.0 gal./hr. to form a spray having a mass median diameter of 15  $\mu$ .

**Step 2**—From Figure 11 the possible combinations of  $M_a/M_l$  and  $\rho_a L$  were selected and tabulated in Table 2.

**Step 3**—Assume:  $\rho_a = 0.003$  g./cc.

Air exit temperature = 80°F.

Liquid tube wall thickness = 0.020 in. The values of the air velocity and viscosity at sonic flow for these conditions, given by reference (16), are:  $v_a = 1,140$  ft./sec. or 34,747 cm./sec.  $\mu_a = 1.848 \times 10^{-4}$  poise or g./((cm.)(sec.))

**Step 4**—Values of  $L$  were calculated by dividing  $\rho_a L$  by the assumed air density.

**Step 5**—The Reynolds numbers in the liquid tubes were then calculated from  $N_{Re} = 4 Q \rho / \mu$

For condition A,  $Q = 0.293$  cc./((sec.)(cm.));  $\rho = 1.0$  g./cc.;  $\mu = 0.009$  g./((cm.)(sec.)); and  $N_{Re} = 130.2$ .

The liquid film thicknesses were calculated from  $t = \left( \frac{3 Q \mu}{\rho g} \right)^{1/3}$ .

**Step 6**—Conditions A through D, Table 2, must be eliminated since the calculated film thickness was less than 0.3 mm. This procedure is recommended to ensure stable liquid flow during atomization.

Condition F must be eliminated since  $N_{Re}$  is greater than 1,000.

**Step 7**—Condition E: Mass of air required,  $M_a/M_l \times M_l = 0.582$  lb./min.

Annular air flow area:

$A = M_a / v_a \rho_a = 0.006549$

Outside diameter of air annulus:

$$D = \left( \frac{A}{0.785} + d^2 \right)^{1/2} = 0.129 \text{ in.}$$

Air supply pressure using Fliegner's equation,  $M_a = \frac{0.533 C_v A P}{(T)^{1/2}}$

and selecting  $C_v = 0.95$

$$P = \frac{M_a \sqrt{T}}{0.533 C_v A} = 68.0 \text{ lb./sq. in., abs.}$$

**Step 8**—From Equation (7)

$$\sigma_m = 2.58 \text{ or } \log \sigma_m = 0.41$$

Other designs close to condition E could be determined by using Equation (5) for values of  $\rho_a L \times 10^4$  g./sq. cm. between 5 and 15.

#### Power Requirements

The power consumption for pneumatic atomizers is generally greater per unit area of surface created than for pressure nozzles or disks. This is usually attributed to the inefficient utilization of the atomizing gas stream. Furthermore since pneumatic atomizers are used primarily for small particle production, their efficiency is further reduced for this reason. More energy is required to produce a spray having a mass median diameter of 10  $\mu$  at a liquid rate of 1.0 gal./hr. than to produce a spray with a mass median diameter of 15  $\mu$  at the same rate.

Based on isothermal expansion of the air from pneumatic atomizers the power consumed for each type studied in this work was calculated and correlated with the drop size produced. The results are summarized in Figure 13, and the corresponding equations for power as a function of mass median diameter are as follows:

#### Converging Nozzle.

$$P_h = (22/\bar{x}_m)^{2.2}, \quad 10 < \bar{x}_m < 22 \mu \quad (9)$$

$$P_h = (9.7/\bar{x}_m)^{18.7}, \quad \bar{x}_m < 8 \mu \quad (10)$$

#### Pneumatic Impingement Nozzle.

$$P_h = (20/\bar{x}_m)^{2.05}, \quad 5 < \bar{x}_m < 20 \mu \quad (11)$$

The curves of Figure 13 and the corresponding equations show rather clearly the extreme difficulty and excessive power required in producing drops in the range of less than 10  $\mu$ . However the importance of nozzle design is also indicated. For a given power consumption the pneumatic impingement nozzle evidently can produce smaller drops than the converging nozzle. One of the great challenges of pneumatic atomization is to design a nozzle which can utilize the energy of the gas stream in the most efficient manner.

#### CONCLUSIONS AND OBSERVATIONS

This study led to drop-size correlations which can be used to determine the conditions of air and liquid streams necessary to produce sprays having mass median diameters between 5 and 30  $\mu$  at liquid rates from 1/2 to 5 gal./hr. The correlations are specific to two types of nozzle designs. When this study had been completed no other design data had appeared in the literature upon which pneumatic nozzle designs could be based for the production of fine sprays. However a large amount of work still remains to be done in the

field; additional studies of other pneumatic nozzle designs, studies of the effect of liquid properties on drop size, studies of the effect of air density on drop size, and studies of other drop size ranges all need to be made. A theory based on these studies is a necessary step to generalization of all experimental results.

Several general observations occurred during this study which are useful. Thus it was interesting to learn that neither pressure nozzles nor high speed rotating disk atomizers could be used to produce sprays having mass median drop diameters of 1 to 15  $\mu$  at liquid rates of 1 gal./hr. with the relative ease that a pneumatic atomizer could perform the operation.

It was observed that drop size varied inversely as the mass ratio of gas to liquid and as the product of gas density (at the point of air and liquid contact) and the length of air to liquid contact periphery as long as the liquid was in the form of a thin stable film. If the liquid film was of nonuniform thickness or if flow rate was nonuniform, sprays having larger-than-expected drop sizes were produced. Pulsating flow evidently produced relatively thick films for atomization which gave larger-than-expected drop size.

It was also observed that pneumatic atomization could be used to produce individual drops having diameters as small as 0.2  $\mu$ ; however the production of sprays with mass median diameters of less than 5 to 8  $\mu$  was quite difficult and required large amounts of energy in the atomizing gas streams. From Figure 13 it is evident that power requirements start to increase exceedingly rapidly at a mass median diameter of 25  $\mu$  for the converging nozzle and at a mass median diameter of 5  $\mu$  for the impinging nozzle. It is possible that redesign of a converging nozzle such that a thin liquid sheet can be contacted by high-velocity air on both sides may produce drop sizes of 7  $\mu$  or less with comparative ease.

The uniformity of sprays increased as the mean drop size decreased. This may be the result of the nearness of approach to direct drop formation from the liquid film in contrast to the usual sequence of film to ligament to drop formation.

Pneumatic atomizers can be used to atomize liquids whose flow properties cause a rapid increase in viscosity with shear. Since the liquid flow channels in a pneumatic nozzle are large in comparison to those in a pressure nozzle the liquid may be brought to the point of atomization with the application of very low shear stresses. For example certain emulsions of polyvinyl chloride can be atomized in a pneumatic nozzle,

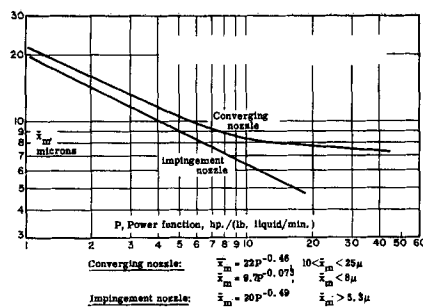


Fig. 13. Power consumption in pneumatic nozzles.

whereas the same emulsions will not flow through a pressure nozzle.

Symmetry must be maintained in the construction and use of a pneumatic atomizer to obtain maximum effectiveness and reproducibility. The converging pneumatic nozzle used in this study did not give reproducible results before positioning screws were installed to permit positive location of the liquid feed tube with respect to the air orifice. The impingement nozzle was very carefully set for symmetrical liquid flow before use.

Several principles to follow for improving the effectiveness of pneumatic atomizer designs are:

1. Nozzles should be designed with a degree of symmetry such that the energy of the expanding gas stream is imparted to the liquid stream as uniformly as possible.

2. Liquid flow conduits should present the liquid to the air stream in the form of a film having a uniform thickness and flowing at a steady, nonpulsing rate.

3. High-velocity air and liquid should be brought into contact over as long a periphery as possible and maintained in contact for as great a period as possible consistent with principle 2.

#### ACKNOWLEDGMENT

This study was supported by the U.S. Army Chemical Corps, Fort Detrick, and by the Engineering Experiment Station of the University of Wisconsin.

#### NOTATION

$A$	= area
$C_v$	= orifice coefficient
$C$	= concentration, g./ml.
$G_a$	= mass velocity of air at nozzle outlet
$L$	= diameter of wetted periphery between air and liquid
$M_a$	= mass rate of air flow from the nozzle
$M_l$	= mass rate of liquid flow from the nozzle
$N_{Re}$	= Reynolds number for film flow inside tubes $-4Q\rho/\mu$
$P_h$	= horsepower/(lb. liquid/min.)
$Q$	= volumetric flow rate per unit of width

$s$	= surface tension
$T$	= absolute air temperature
$t$	= liquid film thickness
$x_l$	= diameter of liquid drop
$x_s$	= diameter of dry particle
$\bar{x}_m$	= mass median spray drop size, $\mu$
$(\bar{x}_m)_s$	= mass median diameter of dry particles
$(\bar{x}_m)_l$	= mass median diameter of liquid drops

#### Greek Letters

$\mu_n$	= viscosity of air
$\rho$	= density of liquid
$\rho_s$	= density of dry solid
$\sigma_m$	= standard deviation, mass basis
$\sigma_n$	= standard deviation, number basis

#### Subscripts

$a$	= air
$l$	= liquid
$m$	= mass
$n$	= number
$s$	= solid

#### LITERATURE CITED

1. Nukiyama, S., and Y. Tanasawa, *Trans. Soc. Mech. Engrs. (Japan)*, **4-6**, Reports 1-6 (1938-40). Translated by E. Hooc for Defence Research Board, Dept. of Nat. Defence, Canada, 10 M-9-47 (393), H.Q. 2-0-264-1 (March 18, 1950).
2. Radcliffe, A., and H. Clare, Nat. Gas. Turb. Establishment (England), *Report No. R.144* (October, 1953).
3. Joyce, J. R., *J. Inst. Fuel*, **4**, 200 (1953).
4. Kim, K. Y., Private communication (1955).
5. Garner, F. H., and V. E. Henny, *Fuel*, **32**, 151 (1953).
6. Golitzine, N., C. R. Sharp, and L. G. Badham, Nat. Aeronaut. Establishment (Canada), *Report 14 ME-186*, Ottawa (1951).
7. Anson, D., *Fuel*, **32**, 39 (1953).
8. Wetzel, R. H., Ph.D. thesis, Univ. Wis. Madison, Wisconsin (1951).
9. Bitron, M. D., *Ind. Eng. Chem.*, **47**, 23 (Jan., 1955).
- 9a. Lewis, H. C., D. G. Edwards, M. J. Goglia, R. I. Rice, and L. W. Smith, *ibid.*, **40**, 67 (1948).
10. Dvork, D., *Ann. Phys.*, **9**, 502 (1880).
11. Foley, J., *Phys. Rev.*, **16**, 449 (1920).
12. Twort, C. C., A. H. Baker, S. R. Finn, and E. O. Powell, *J. Hygiene*, **40**, 253 (1940).
13. Friedman, S. J., and C. O. Miller, *Ind. Eng. Chem.*, **33**, 885 (1941).
14. Whytlaw-Gray, R., and H. S. Patterson, "Smoke: A Study of Aerial Disperse Systems," Edward Arnold & Co., London, England (1932).
15. Rosebury, T., "Experimental Air-Borne Infection," Chap. 7, Williams and Wilkins, Baltimore, Maryland (1947).
16. "Handbook of Supersonic Aerodynamics," NAVORD Rept. 1488, Vol. 5, U.S. Gov't. Printing Office (Aug., 1953).

Manuscript received January 10, 1959; revision received July 21, 1960; paper accepted July 25, 1960. Paper presented at A.I.Ch.E. Cincinnati meeting.